# Low Loss InP C-Band IQ Modulator with 40GHz Bandwidth and 1.5V Vπ

**Gregory Letal[1], Kelvin Prosyk[1], Ron Millett[1], David Macquistan[1], Stéphane Paquet[2], Olivier Thibault-Maheu[2], Jean-Frédéric Gagné[2], Pierre-Louis Fortin[2], Reza Dowlatshahi[3], Brian Rioux[3], Tony SpringThorpe[3], Matt Hisko[3], Rubin Ma[3], Ian Woods[1]**

[1] *TeraXion, 232 Herzberg Rd, Ottawa, Ontario, Canada K2K 2A1*

[2] *TeraXion, 2716 Einstein Street, Quebec, Quebec, Canada G1P 4S8*

[3] *Canadian Photonics Fabrication Centre, Building M-50, Rm C133, 1200 Montreal Road, Ottawa, Ontario, Canada, K1A 0R6*

gletal@teraxion.com

**Abstract:** Design and fabrication improvements to InP optical IQ modulators resulted in a reduced Vπ of 1.5V while maintaining 40GHz bandwidth and loss <7.5dB over C-band. Dual polarization QPSK constellations using 3Vpp drive are presented.

**OCIS codes:** (250.4110) Modulators; (130.0250) Optoelectronics

## 1. Introduction

Broadband InGaAsP/InP Mach Zehnder modulators (MZMs) with a Vπ of 2.5V have been developed by our group for use in compact transmitters in the ITU-T single-mode fiber spectral C-band [1]. The concept was extended to an optically nested configuration to form an in-phase quadrature modulator (IQM) [2,3].

A reduction from 5V to 3V in the required peak-to-peak (2xVπ) drive voltage can cut the power consumption of an amplifier by 60%, thereby keeping total driver power for a four-channel dual-polarization quadrature phase shift keyed (DP-QPSK) transmitter to within 1-2W, depending on the bias configuration of the drivers. Consequently, we have further optimized our previous IQM design [2]. The new chip, while retaining the same 1.08 x 11 mm footprint, is capable of < 6.5dB insertion loss (IL) over the 40nm C-band with a Vπ of 1.75V. By altering the operating conditions slightly, the same design can achieve a Vπ of 1.5V with an IL of < 7.5dB.

## 2. Design

Indium phosphide MZM design is a compromise between Vπ, IL, bandwidth and chip length. In addition, for a given design, increasing the DC bias across the multi-quantum well (MQW) core can decrease Vπ, but can also result in voltage-dependent absorption that adversely affects IL and unpredictably degrades extinction ratio (ER). To reduce the Vπ without a detrimental effect on other parameters, it is necessary to increase the slope of the index change as a function of applied voltage (electro-optic efficiency or EOE) for a given TWE loading capacitance [4].

InGaAsP layers were grown on three-inch (100)-oriented Fe:InP wafers in a multi-wafer MOCVD reactor. Controls such as multiple point *in-situ* reflectance and emission compensated pyrometry were introduced. A non-contact 5X ASML i-line stepper was used for photolithography, giving high alignment accuracy and uniformly vertical photoresist patterns. Optical waveguides were etched in a SPTS inductively coupled plasma etch cluster tool using a customized bromine-based chemistry, allowing the photoresist pattern to be replicated into the semiconductor and resulting in smooth, vertical sidewalls on the optical waveguides.

With the improvements in growth, the number of quantum wells could be increased by 45%, from 22 to 32, increasing the optical confinement by 25%. A cross section of the 32-well core butt-joined to the re-optimized bulk core of the SSC is shown in Fig. 1. Smooth sidewalls allowed for narrow waveguides without introducing appreciable optical scattering losses. With the loading capacitance thereby reduced, the waveguide electrode mark-to-space ratio in the TWE, and hence EOE, could therefore be increased by 30% without impacting the bandwidth.

With an aggregate increase in EOE of 63%, our previously reported Vπ of 2.5V could be reduced to 1.5V while maintaining similar performance in other regards. Alternately, the DC bias applied to the TWE could be reduced, in order to target a 1.75V Vπ operating point with a further reduction in insertion loss.

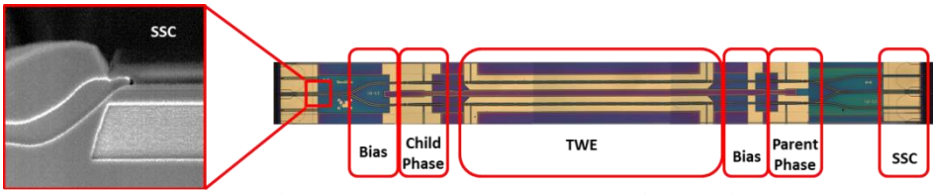


Fig. 1. Cross-sectional SEM showing the butt-joint of the SSC and MQW cores and an image of the top of the chip.

### 3. Chip Results at 1.75V Vπ

Typical DC test results at 40°C are shown in Figure 2. The bias of the TWE ranged from 2.75V to 7V as it was adjusted for a constant Vπ of 1.75V over the 1528 to 1567nm wavelength range. Each child MZM was swept in turn with a differential voltage across the TWE, similar to what would be applied during dynamic operation, while the other child was switched off. The independent DC phase control electrodes were set so the IQM was in the correct quiescent phase state for QPSK operation. The IL corresponds to the sum of output power as each child MZM was switched from the off state to the on state, with 3 dB subtracted from the result to account for the quadrature combination of the parent interferometer (max/max/max). IL < 6.5dB and ER > 25dB were observed.

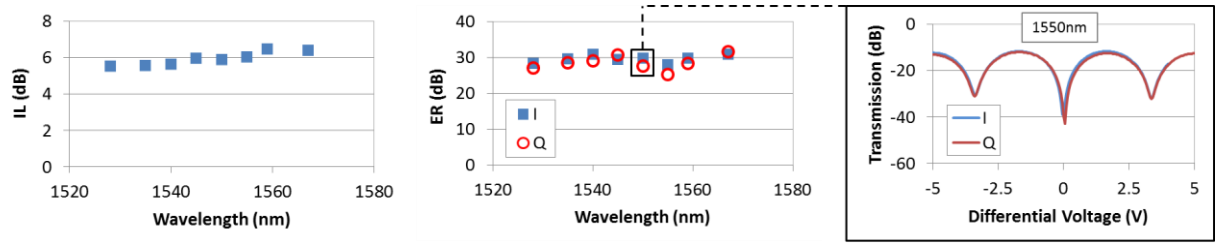


(a) (b) (c)

Fig. 2. DC characteristics of an IQM set to its QPSK operating state and 1.75V Vπ: (a) IL; (b) child MZM ER; and (c) child MZM switching curves at 1550nm.

### 4. Chip-on-Carrier Results at 1.5V Vπ

An IQM chip was mounted on an AlN carrier (CoC) along with 50-Ohm CPW RF interconnect waveguides and terminations. The temperature of the carrier was increased to 60°C and the DC bias was adjusted for a Vπ of 1.5V. Pulsed measurements of the TWEs were performed so as to avoid an artificially high DC power from dissipating in the terminations when a differential voltage was applied. The results are shown in Fig. 3. The device was tested in 1nm steps in order to verify that the ER was not unduly degraded by the elevated DC bias. Noise caused by the pulse window also perturbed the measurement. IL < 7.5dB and ER > 21dB were observed. EO response and S11 were collected, shown in Fig. 4(a).

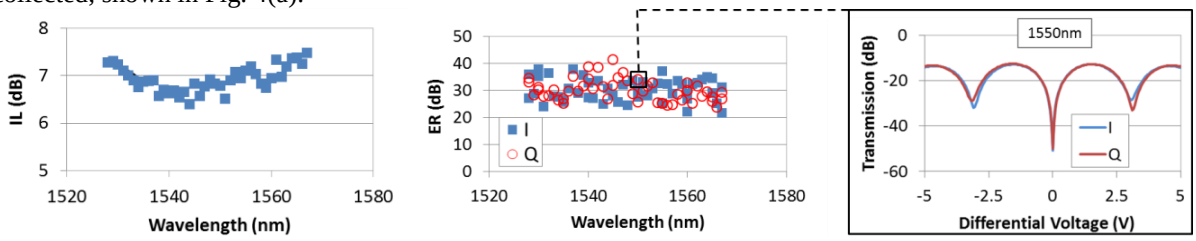


(a) (b) (c)

Fig. 3. DC characteristics of an IQM set to its QPSK operating state and 1.5V Vπ: (a) IL; (b) child MZM ER; and (c) child MZM switching curves at 1550nm.

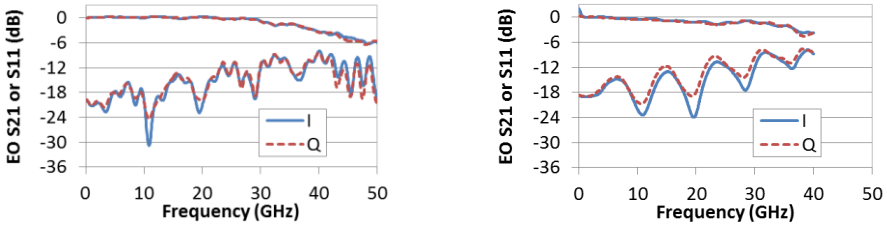


(a) (b)

Fig. 4. Results of small signal modulation for (a) the CoC from Fig. 3; and (b) the same CoC built into a DP-QPSK sub-assembly. The sub-assembly was measured using a different network analyzer, which was limited to 40GHz.

### 5. DP-QPSK Sub-assembly with 3V Drive

The CoC in section 3 along with a second sample was built into a small (24.25mm x 7.5mm) prototype evaluation sub-assembly which included all the coupling optics and RF interconnects required for 112 Gb/s DP-QPSK, as shown in Fig. 5. Bulk micro-optics were used to split, route, rotate and recombine the light. Conduction-backed coplanar waveguides (CB-CPWs) carried the input electrical signal.

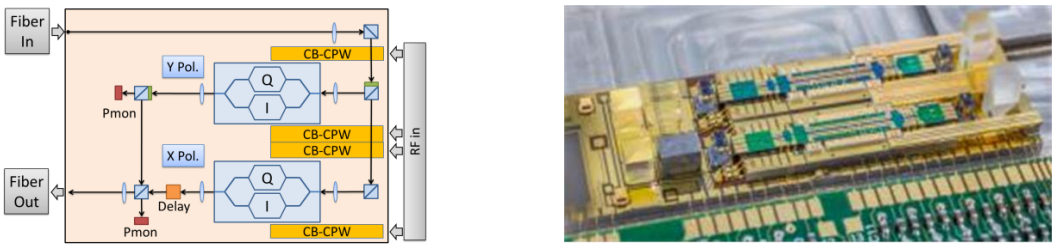


Fig. 5. DP-QPSK sub-assembly.

The sub-assembly was optically coupled to fiber with collimating lens assemblies. The modulators were driven with a PRBS pattern of $2^9$-1 at 28 Gbaud/s, which was delayed to provide four independent signals. The PRBS output and gain of the OA3MHQM Centellax driver were adjusted to provide 3V peak-to-peak signals for 2x$V\pi$ operation of the IQMs. The optical output was collected with a Tektronix lightwave signal analyzer (OM4106D).

The small signal response is shown in Fig. 4(b). Constellation and extracted eye diagrams are shown for both polarizations at 1550nm operating wavelength in Fig. 6. The error vector magnitude (EVM) is summarized in Table 1. In all cases it was < 11%. There was a slight ~1dB power imbalance between X and Y channels that will be addressed in future builds.

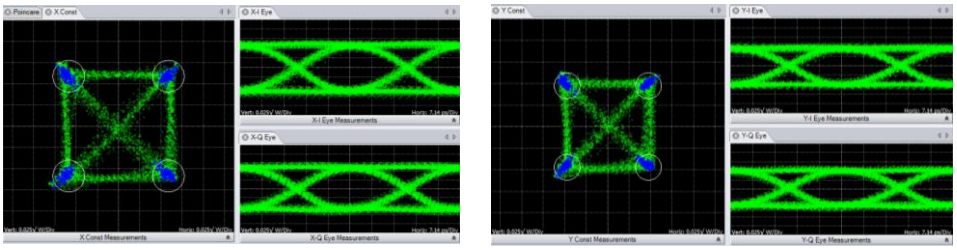

(a) (b)

Fig. 6- Sub-assembly constellation diagram and both I and Q eye diagrams for (a) the X-polarized and (b) the Y-polarized constellations.

Table 1. Summary of EVM values

| Wavelength | X Constellation EVM | Y Constellation EVM |
|---|---|---|
| 1528 | 10.9 | 10.59 |
| 1550 | 9.48 | 10.66 |
| 1565 | 9.23 | 10.18 |

## 6. Summary

In an effort to reduce the size and power consumption of DP-QPSK transmitters, and taking advantage of advances in both growth and photolithography technology, an improved InP-based IQ modulator was developed. The MQW waveguide core, travelling wave electrode and spot-size converter were re-optimized, resulting in a reduction of the DP-QPSK peak-to-peak modulation voltage from 5V to 3V ($V\pi$ decreased from 2.5V to 1.5V) while reducing the optical insertion loss to < 7.5dB. The chip dimensions were unchanged, and the optical bandwidth, RF bandwidth, and extinction ratio remained comparable to the previous higher voltage design.

## 7. References

[1] K. Prosyk, A. Ait-Ouali, C. Bornholdt, M. Gruner, M. Hamacher, D. Hoffmann, R. Kaiser, R. Millett, K.-O. Velthaus, I. Woods, "High performance 40GHz InP Mach-Zehnder modulator", OFC/NFOEC Technical Digest, OW4F.7, 2012.

[2] K. Prosyk, T. Brast, M. Gruner, M. Hamacher, D. Hoffmann, R. Millett, and K.-O. Velthaus, "Tunable InP-based Optical IQ Modulator for 160 Gb/s", ECOC 2011, Th.13.A.5.

[3] E. Rouvalis, C. Metzger; A. Charpentier; T. Ayling. S. Schmid, M. Gruner, D. Hoffmann, M. Hamacher, G. Fiol, M. Schell, "A Low Insertion Loss and Low $V_\pi$ InP IQ Modulator for Advanced Modulation Formats", ECOC 2014, Tu.4.4.1

[4] R. G.Walker and J. Heaton, "Gallium arsenide modulator technology," in Broadband Optical Modulators—Science, Technology and Applications, A. Chen and E. J. Murphy, Eds. Boca Raton, FL, USA: CRC Press, 2012, ch. 8, pp. 207–221.